



© 2023 Geological Society of America. For permission to copy, contact editing@geosociety.org

Manuscript received 14 June 2023 Revised manuscript received 22 August 2023 Manuscript accepted 4 September 2023

Published online 21 September 2023

Oceanic serpentinites: A potentially critical reservoir for deep nitrogen recycling

Kan Li^{1,*}, Amber Jie Yu¹, Peter H. Barry², and Long Li¹

Department of Earth and Atmospheric Sciences, University of Alberta, Edmonton, AB T6G 2E3, Canada

²Marine Chemistry & Geochemistry Department, Woods Hole Oceanographic Institution, Woods Hole, Massachusetts 02543, USA

ABSTRACT

Serpentinized oceanic peridotites might be an important reservoir delivering volatile elements including nitrogen (N) into the mantle via subduction. To determine N sources and estimate the budget of alteration-added secondary N in the oceanic mantle peridotite reservoir, we examined oceanic serpentinites from four Ocean Drilling Program (ODP) sites in the Pacific and Atlantic Oceans. Our results showed that, despite large variation in serpentinization condition (high temperatures up to >350 °C at Holes 895D, 1271B, and 920D; low temperatures <150 °C at Hole 1274A), serpentinites from all sites displayed ubiquitous and similar magnitude of N enrichment (3.2-18.6 ppm) from sediments/seawater sources ($\delta^{15}N = -3.3\%$ to +4.4%), and these values were significantly elevated relative to the low N concentration (0.04–2.0 ppm) and δ^{15} N value ($-5\%c \pm 2\%c$) of the depleted mantle. Based on these data, the serpentinized oceanic mantle is estimated to contribute 0.4 ± 0.2 – $14.7 \pm 6.9 \times 10^9$ mol N annually to global subduction zones. Although this flux is smaller than that of subducting sediments (57×10^9 mol·yr⁻¹), comparison between oceanic serpentinites and meta-serpentinites from subduction zones suggests that N can be effectively retained in serpentinites during prograde metamorphism. This implies that the serpentinized slab mantle could be a critical reservoir to deliver N enriched in 15N to the mantle (at least 70 km depth) and potentially to the deepest portions of the mantle sampled by deep-rooted mantle plumes.

INTRODUCTION

Understanding the nitrogen (N) budget of subducting slabs is essential for quantifying deep N recycling. The major components in subducting slabs are sediments, altered oceanic crust (AOC), and the mantle beneath the slab. Seafloor sediments are best characterized by enrichment in N (N = 5-2400 ppm; $\delta^{15}N = -1\%$ to +10%; Sadofsky and Bebout, 2004; Li and Bebout, 2005), whereas the igneous components (fresh basalt, gabbro, and peridotite) have significantly lower N contents, derived from the depleted mantle (DM) $(N = 0.04-2.0 \text{ ppm}; \delta^{15}N = -5\% \epsilon \pm 2\% \epsilon)$ (Marty, 2012; Johnson and Goldblatt, 2015; Bekaert et al., 2021). Recent studies have shown that submarine hydrothermal alteration

Kan Li https://orcid.org/0000-0002-1161-8434 *Current address: Marine Chemistry & Geochemistry Department, Woods Hole Oceanographic Institution, Woods Hole, Massachusetts 02543, USA; kan3@ualberta.ca

can fix significant amounts of sedimentary/seawater NH_4^+ by K- and/or Na-bearing secondary minerals (e.g., clay and albite; Honma and Itihara, 1981; Y.H. Li et al., 2021), particularly in upper volcanic and lower intrusive sections (N = 1.3–48.4 ppm; $\delta^{15}N = -20\%$ to +7%; Li et al., 2007; Li and Li, 2023a, 2023b, and references therein). Due to the large mass of AOC entering trenches, it has been demonstrated to be an important N reservoir, along with sediments, for deep N recycling (e.g., Li et al., 2007; Busigny et al., 2011).

Compared with AOC, the mantle beneath the slab is even more massive. Serpentinization of the slab mantle, driven by fluid introduced by detachment and slab bending–related faults, can enrich volatile components (e.g., carbon; Alt et al., 2013) in subducting slabs to participate further in deep recycling to the subarc depth (Deschamps et al., 2013) and even beyond to the deeper mantle (Kendrick et al., 2017). However, the N storage capacity in oceanic serpentinites has not been systematically examined, apart

from three samples from the Southwest Indian Ridge (N = 2.0–2.9 ppm and δ^{15} N = +6.3% to +7.5%; Philippot et al., 2007). A recent study of serpentinized slab mantle materials subducted to \sim 70 km depth from the Ligurian Alps and Bètic Cordillera reported much higher N contents (1.3-20.6 ppm) and demonstrated negligible N loss during prograde metamorphism (Halama et al., 2014). This highlights serpentinites as a potential host for deep N recycling (Halama et al., 2014). However, it is uncertain whether N enrichment in these meta-serpentinites occurred during presubduction hydrothermal alteration (i.e., external N from seawater/sediments) or within the subduction channel through intraslab metasomatic addition (i.e., internal slab N), since both have been observed in meta-basalts (Halama et al., 2014; K. Li et al., 2021). The N characteristics of pre-subduction oceanic serpentinites can thus provide a key reference point for understanding N behavior in subduction zones recorded by metaserpentinites as well as for quantifying the N budget in global subducting serpentinites; however, these key samples remain poorly studied.

Here, we report bulk-rock N concentrations and isotope compositions of oceanic serpentinites (n=26) from four Ocean Drilling Program (ODP) sites (Fig. 1A), including Hole 895D at the Hess Deep (n=8), Holes 1271B (n=5) and 1274A (n=6) at the 15°20′N fracture zone in the Mid-Atlantic Ridge, and Hole 920D (n=7) at the Mid-Atlantic Ridge \sim 35 km south of the Kane Fracture Zone, together with pure serpentine vein minerals (n=2) from Hole 895D. These data allow for a first assessment of N uptake by oceanic serpentinites during hydrothermal alteration.

SAMPLE DESCRIPTION

Serpentinites at these four sites were overthrusted onto the seafloor by either crustal thinning along low-angle detachment faults or propagating rifts (Fig. 1B; Alt et al., 2013). The studied samples are altered (~70%–100%)

CITATION: Li, Kan, et al., 2023, Oceanic serpentinites: A potentially critical reservoir for deep nitrogen recycling: Geology, v. 51, p. 1096–1100, https://doi.org/10.1130/G51464.1

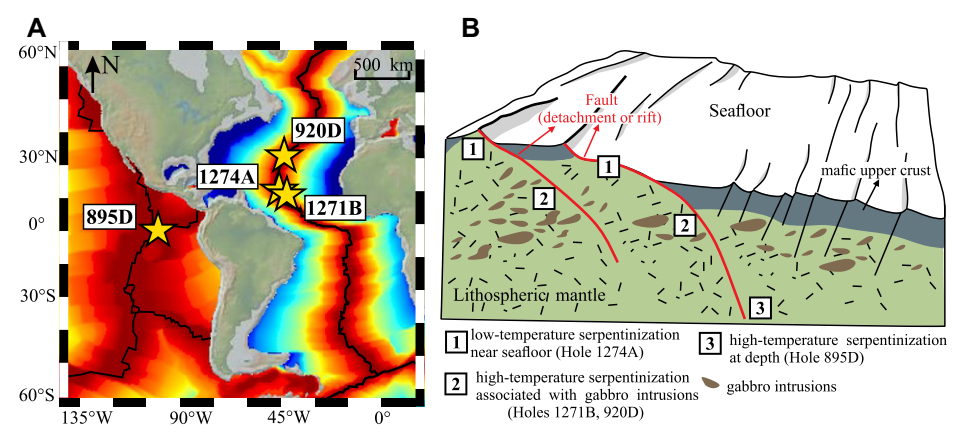


Figure 1. (A) Map of oceanic crust in Pacific and Atlantic Oceans showing sample sites (Geo-MappApp). (B) Schematic diagram showing various serpentinization conditions of studied samples.

harzburgites or dunites with a secondary mineral assemblage dominated by serpentine and minor magnetite (S1 in the Supplemental Material¹). The samples commonly contain thin ($<\sim$ 0.1

'Supplemental Material. Detailed sample descriptions (S1), description of high-temperature and low-temperature serpentinization (S2), analytical methods (S3), two-component mixing model (S4), estimation of nitrogen input flux of the serpentinized slab mantle (S5), Figure S1 (compilation of nitrogen concentration data of altered oceanic crust), Figure S2 (two-component mixing model), and Figure S3 (temperature and pressure conditions of meta-basalts, meta-gabbros and meta-serpentinites). Please visit https://doi.org/10.1130/GEOL.S.24085755 to access the supplemental material, and contact editing@geosociety.org with any questions.

mm) veins dominantly composed of serpentine \pm magnetite. Thick veins (>0.5 mm) are rare, but two 1–2-mm-wide pure fibrous serpentine veins from Hole 895D were successfully sampled by microdrilling.

Following Alt et al. (2013), the oceanic serpentinites from four sites were classified into two groups based on the serpentinization temperatures (T) (Supplemental Material S2): (1) high-T serpentinization at depth, where serpentinization at Holes 1271B and 920D predominantly occurred at >350 °C by heat transfer from gabbroic intrusions (Fig. 1B; Alt et al., 2007, 2013), while serpentinization at Hole 895D occurred at 200–400 °C by the injection of seawater into hot peridotites at a depth of \sim 5

km during the rifting process (Fig. 1B; Mével and Stamoudi, 1996); and (2) low-*T* serpentinization near the seafloor, where serpentinization at Hole 1274A occurred at <150 °C following exposure of peridotites at the seafloor by faulting (Fig. 1B; Alt et al., 2007).

RESULTS

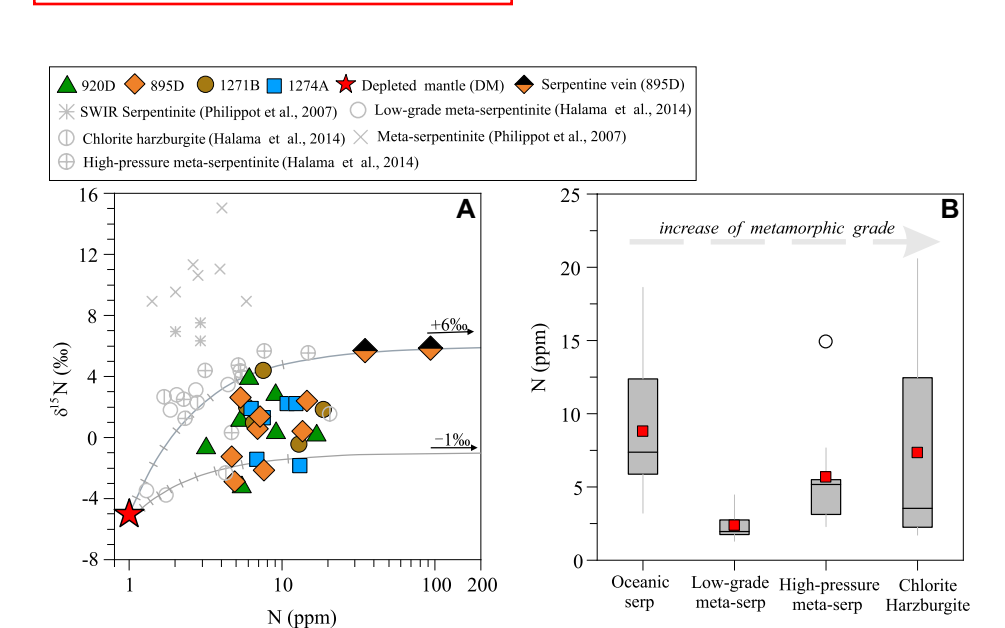
Serpentinites from the four sites displayed large ranges of N concentrations (3.2–18.6 ppm; average: 8.8 ± 4.1 ppm, 1σ) and $\delta^{15}N$ values (-3.3% to +4.4%; average: +0.7% $\pm 2.0\%$, 1σ) (Fig. 2A; Table S1; see Supplemental Material S3 for methods), which were consistently elevated relative to the DM. No downhole trend was observed for N concentrations and $\delta^{15}N$ values. The two serpentine veins from Hole 895D showed much higher N concentrations (34.9–94.0 ppm) and slightly higher $\delta^{15}N$ values (+5.7% to +5.9%) than the bulk-rock data.

DISCUSSION

Ubiquitous N Enrichment in Oceanic Serpentinites

The N concentrations (3.2–18.6 ppm) of the serpentinites from the four ODP sites demonstrate that significant amounts of secondary N can be incorporated into altered ultramafic mantle-sourced rocks. The magnitude of N enrichment in serpentinites is comparable to that in AOC (mostly <20 ppm; Fig. S1; Li et al., 2007; Li and Li, 2023a, 2023b).

While N enrichment into AOC is mainly due to substitution of NH_4^+ for K^+ and (to a lesser extent) Na^+ in the crystal lattice of sec-



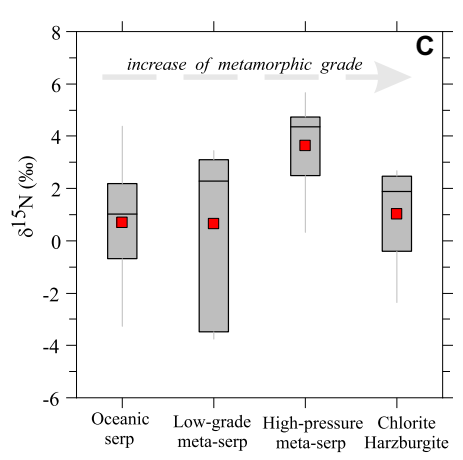


Figure 2. (A) $N-\delta^{15}N$ diagram showing that oceanic serpentinite (serp) data (error bars are smaller than symbol size) can be explained by adding secondary N ($\delta^{15}N = -1\%$ to +6%) into depleted mantle (DM) (with N = 1.0 ppm, which is average of total range of 0.04–2.0 ppm; $\delta^{15}N = -5\%$; Supplemental Material S4 [see text footnote 1]). Fraction of secondary N in mixture is marked on mixing curve with 10% increments. For comparison, oceanic serpentinite data from Southwest Indian Ridge (SWIR) and meta-serpentinite data are also shown. (B–C) Box plots comparing N concentrations and $\delta^{15}N$ values of rocks along prograde metamorphic path from oceanic serpentinites, low-grade meta-serpentinites, and high-pressure meta-serpentinites to chlorite harzburgite. Boxes—interquartile range; horizontal line—median value; red-filled square—mean value; empty circle—outliers.

ondary minerals (e.g., clay minerals and albite; Honma and Itihara, 1981; Y.H. Li et al., 2021), this mechanism is less prevalent in serpentinites due to the lack of K- and Na-bearing minerals in these rocks, as revealed by their negligible K₂O and Na₂O contents (e.g., Mével and Stamoudi, 1996). Instead, the high N concentrations in the two serpentine veins (Table S1) indicate that serpentine (as the predominant phase) is likely the major N-hosting mineral in serpentinites. The uptake of NH₄⁺ by serpentine is more likely to occur via adsorption rather than cation substitution. Adsorption of large cations (e.g., Cs⁺; 1.88 Å; Shannon and Prewitt, 1969) with an ionic radius similar to NH_4^+ (1.67 Å; Sidey, 2016) by serpentine has been previously reported (Lafay et al., 2016). The observed N enrichment in serpentine suggests that N may occur as a trace element in many more minerals than previously thought.

The N concentrations and δ15N values in the serpentinites can be readily explained by a two-component mixing model (Supplemental Material S4 and Fig. S2) between the DM and secondary N with a δ^{15} N range of -1% to +6%(Fig. 2A), which is consistent with a N source from sediments and seawater-derived hydrothermal fluids, where variable $\delta^{15}N$ values of NH_4^+ have been observed (-1% to +10%; Sadofsky and Bebout, 2004; Li and Bebout, 2005; Charoenpong, 2019). Data from the two pure serpentine veins, which precipitated directly from hydrothermal fluids, are considered to best represent the signature of secondary N in fluids. These data plot on the upper mixing line in Figure 2A, lending credence to the assumed secondary N source with a δ^{15} N value of +6%o. Additionally, the variable δ^{15} N values of serpentinites could also be a result of heterogeneous incorporation of NH₄+ from hydrothermal fluids with variable $\delta^{15}N$ values at multiple alteration stages. Nevertheless, mass-balance calculations indicate that 66%-94% of the N in these oceanic serpentinites is secondary.

Equivalent N Enrichments in Low-T and High-T Serpentinites

Although serpentinization T varied significantly among the four ODP sites, no obvious intersite differences were observed in either N concentrations or $\delta^{15}N$ values (Fig. 2A). Because N availability is the primary factor controlling the enrichment of N in AOC (Li and Li, 2023b), it is not surprising that we observed significant N enrichments in the low-T serpentinites, as abundant NH₄⁺ is available in the near-seafloor environment. It is however interesting that we observed equivalent N enrichment by high-T serpentinization at depth. This implies that either (1) sufficient surface NH₄⁺ can be delivered to depth by seawater-derived fluids via deep faults to facilitate N assimilation, or (2) high-T serpentinization can more efficiently assimilate N if the fluid NH₄+ is limited. Either way, the consistently high N concentrations in all three high-T serpentinites suggest that the serpentinized mantle rocks at depth contain significant amounts of N. Notably, the high hydrogen fugacity and strongly alkaline conditions in serpentinization environments (especially at T < 250 °C; McCollom and Bach, 2009) are able to produce NH₄⁺ characterized by extremely low $\delta^{15}N$ values (-5% to -20%; due to abiotic N_2 reduction by H₂; Li et al., 2007; Li and Li, 2023b) and high δ^{15} N values (>+10% $_{e}$; due to large fractionation between NH₃ and NH₄+; Li et al., 2012), respectively, which were, however, not observed in our samples. This suggests that these two parameters may not be key factors controlling the variability of δ^{15} N values in serpentinites, but they are worth investigating in future studies.

Nitrogen Retention in Serpentinites During Subduction

Our systematic characterization of N concentrations and $\delta^{15}N$ values in oceanic serpentinites allowed us to further assess the N behavior within subduction channels. We compared the new oceanic serpentinite data with their metamorphic equivalents (i.e., meta-serpentinite; Fig. 2), including low-grade samples (<0.5 GPa and <300 °C) from the Erro Tobbio and Monte Nero units (Ligurian Alps), high-pressure samples (550-600 °C and 2.0-2.5 GPa) that experienced partial antigorite dehydration in the Erro Tobbio unit, and the chlorite harzburgite (>650–700 °C and \sim 2 GPa) that formed by complete antigorite dehydration in the Cerro del Almirez unit (Bètic Cordillera) (Halama et al., 2014). The protoliths of these meta-serpentinites had experienced low-T to high-T serpentinization in seafloor settings (Halama et al., 2014). Therefore, the oceanic serpentinites studied here can be used as a reference for their protoliths.

As illustrated in Figure 2, the meta-serpentinite data from Halama et al. (2014) largely overlap with the oceanic serpentinite data here in both N concentrations and $\delta^{15}N$ values. Crucially, the progressive decrease of N concentrations and increase of $\delta^{15}N$ values corresponding to prograde metamorphic N devolatilization (Bebout and Fogel, 1992) were not observed in the meta-serpentinites (Figs. 2B and 2C). Nevertheless, the meta-serpentinites from the Erro Tobbio units studied by Philippot et al. (2007) showed consistently lower N concentrations and higher $\delta^{15}N$ values (Fig. 2A), which are consistent with the isotopic effect of partial N loss (Bebout and Fogel, 1992). However, this partial N loss may in fact have been the result of the 450 °C preheating treatment of samples employed by Philippot et al. (2007), which can remove various amounts of N in secondary minerals (Bebout et al., 2018; L. Li et al., 2021). Overall, the comparison between oceanic serpentinites and their metamorphic equivalents

suggests that serpentinites are capable of retaining N within a subduction zone during prograde metamorphism. In contrast, eclogite-facies meta-basalts and meta-gabbros with similar metamorphic conditions (Fig. S3) showed variable degrees of N loss under eclogite-facies metamorphism (Li and Li, 2023a, 2023b). Together, these findings highlight that meta-serpentinites retain N during deep subduction more efficiently than meta-basalts and meta-gabbros.

IMPLICATIONS FOR DEEP N RECYCLING

Our data demonstrate that N can be enriched in mantle rocks via serpentinization, not only during low-T alteration near the seafloor, but also at depth, as hydrothermal fluid penetrates along faults. Seaward trenches and slab bending can produce faults that allow deep penetration of fluids into the oceanic lithospheric mantle, resulting in serpentinization (Grevemeyer et al., 2018). If we assume the degree of serpentinization is between $\sim 1\%$ and 30% in the uppermost 10 km of the oceanic slab mantle (Supplemental Material S5), together with the average N concentration (8.8 \pm 4.1 ppm) of oceanic serpentinites obtained in this study, the global trench length of 44,500-60,000 km, an average convergence rate of 0.05 m·yr⁻¹, and dry density of 2.6 g·cm⁻³ (Supplemental Material S5), we can calculate an N flux of 0.4 ± 0.2 – $14.7 \pm 6.9 \times 10^9 \text{ mol·yr}^{-1}$ into global subduction zones. This estimate overlaps with previous estimates $(0.4-9.1 \times 10^9 \text{ mol·yr}^{-1}; \text{ Halama})$ et al., 2014; Bekaert et al., 2021) employing a serpentinization degree of ${\sim}4\%$ to 100% and a conservative N concentration (\sim 2 ppm) for the uppermost 10 km of serpentinized slab mantle, but it extends toward higher values.

Notably, our new N input flux estimate for the slab mantle is the same magnitude as estimations from global AOC, including the upper volcanic (i.e., basalts; $3.7 \pm 0.3 \times 10^9$ mol·yr⁻¹) and lower intrusive sections (i.e., sheeted dikes and gabbros; $17.0^{+1.0}_{-1.3}$ – $26.2 \pm 2.3 \times 10^9$ mol·yr⁻¹; Li and Li, 2023a, 2023b) (Figs. 3A and 3B). Taken together, these three igneous components contribute a total N flux of $21.0^{+1.0}_{-1.3}$ $-44.6 \pm 7.2 \times 10^9$ mol·yr⁻¹ into the trench (Fig. 3B), which is \sim 37%–78% of the amount that subducting sediments contribute (57 \times 10⁹ mol·yr⁻¹; Fig. 3B; Busigny et al., 2003). However, meta-igneous components inside subduction channels have a much stronger N retention capability versus metasediments, and they can also act to re-fix N released from metasediments (Halama et al., 2010, 2014; Cannaò et al., 2020; K. Li et al., 2021); therefore, the igneous components may in fact dominate deep recycling of surface N (Li et al., 2019). Critically, among the igneous components of subducting slabs, the meta-serpentinites show the highest N retention capability, highlighting the fact that

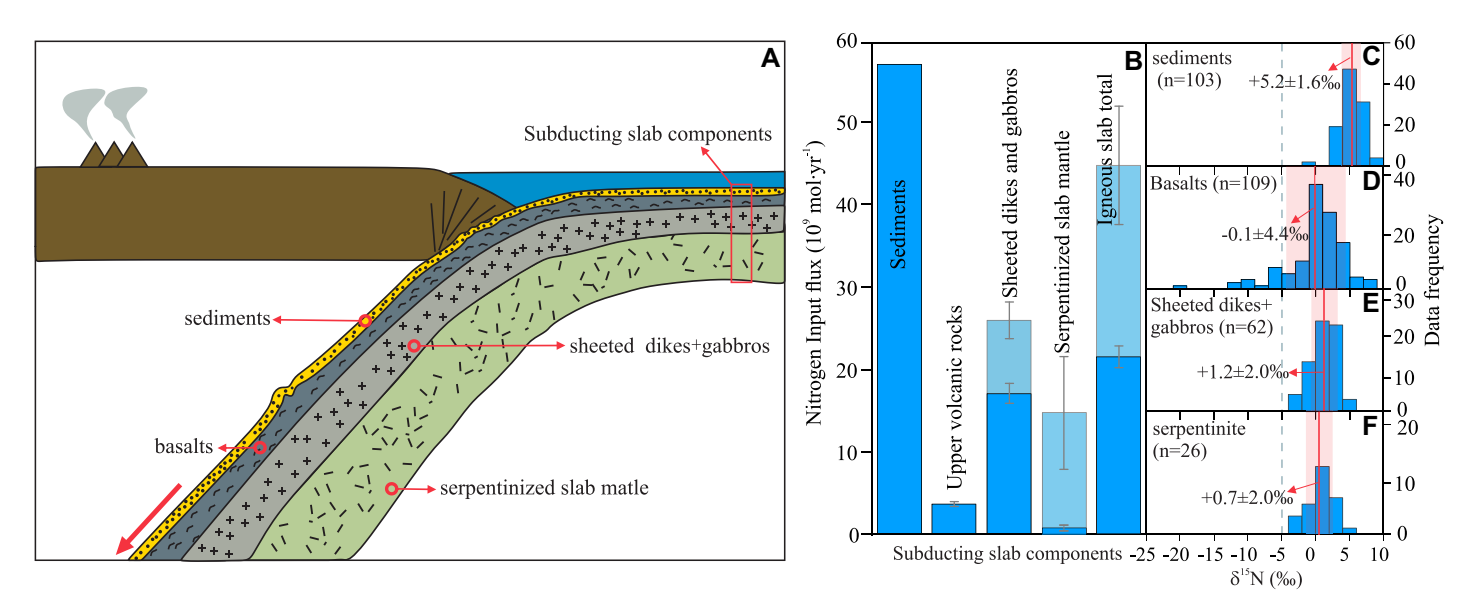


Figure 3. (A) Schematic diagram (not to scale) showing four lithological components of subducting slabs. (B) Estimated global N input flux of sediments, basalts, sheeted dikes and gabbros, serpentinized slab mantle, and total of igneous slab. Shaded blue boxes represent upper-end estimation of N input fluxes. (C–F) Histograms showing δ^{15} N values of four lithological components of subducting slabs. Red solid lines and shaded boxes mark average and 1 standard deviation of compiled δ^{15} N data. Gray dashed line marks δ^{15} N value of depleted mantle (DM) (-5%).

serpentinized slab mantle could be a critical N reservoir facilitating transport of surface N into the deeper mantle.

When comparing the average $\delta^{15}N$ values of the four lithological components of subducting slabs with the DM (Figs. 3C–3F), the serpentinized slab mantle ($+0.7\%c \pm 2.0\%c$) consistently carries N enriched in ^{15}N into subduction zones, in parallel with the upper volcanic ($-0.1\%c \pm 4.4\%c$) and the lower intrusive sections ($+1.2\%c \pm 2.0\%c$) of AOC, and seafloor sediments ($+5.2\%c \pm 1.6\%c$; Sadofsky and Bebout, 2004; Li and Bebout, 2005). However, the high retention of N in meta-serpentinites reinforces its critical role in conveying ^{15}N -enriched signatures to the deeper Earth, as observed in deep-rooted mantle plumes ($+3\%c \pm 2\%c$; Dauphas and Marty, 1999; Barry and Hilton, 2016).

ACKNOWLEDGMENTS

This work was supported by a Natural Sciences and Engineering Research Council of Canada Discovery grant to L. Long. This paper benefitted from constructive comments by Ralf Halama, Vincent Busigny, Michael W. Förster, and two anonymous reviewers. We thank editor Marc D. Norman for efficient handling of the manuscript.

REFERENCES CITED

Alt, J.C., Shanks, W.C., Bach, W., Paulick, H., Garrido, C.J., and Beaudoin, G., 2007, Hydrothermal alteration and microbial sulfate reduction in peridotite and gabbro exposed by detachment faulting at the Mid-Atlantic Ridge, 15°20'N (ODP Leg 209): A sulfur and oxygen isotope study: Geochemistry, Geophysics, Geosystems, v. 8, Q08002, https://doi.org/10.1029/2007GC001617.

Alt, J.C., Schwarzenbach, E.M., Früh-Green, G.L., Shanks, W.C., III, Bernasconi, S.M., Garrido, C.J., Crispini, L., Gaggero, L., Padrón-Navarta, J.A., and Marchesi, C., 2013, The role of serpentinites in cycling of carbon and sulfur: Seafloor serpentinization and subduction metamorphism: Lithos, v. 178, p. 40–54, https://doi.org/10.1016/j.lithos.2012.12.006.

Barry, P., and Hilton, D., 2016, Release of subducted sedimentary nitrogen throughout Earth's mantle: Geochemical Perspectives Letters, v. 2, p. 148–159, https://doi.org/10.7185/geochemlet.1615.

Bebout, G.E., and Fogel, M.L., 1992, Nitrogen-isotope compositions of metasedimentary rocks in the Catalina Schist, California: Implications for metamorphic devolatilization history: Geochimica et Cosmochimica Acta, v. 56, p. 2839–2849, https://doi.org/10.1016/0016-7037(92)90363-N.

Bebout, G.E., Banerjee, N., Izawa, M., Kobayashi, K., Lazzeri, K., Ranieri, L., and Nakamura, E., 2018, Nitrogen concentrations and isotopic compositions of seafloor-altered terrestrial basaltic glass: Implications for astrobiology: Astrobiology, v. 18, p. 330–342, https://doi.org/10.1089/ast.2017.1708.

Bekaert, D.V., Turner, S.J., Broadley, M.W., Barnes, J.D., Halldórsson, S.A., Labidi, J., Wade, J., Walowski, K.J., and Barry, P.H., 2021, Subduction-driven volatile recycling: A global mass balance: Annual Review of Earth and Planetary Sciences, v. 49, p. 37–70, https://doi.org/10.1146/annurev-earth-071620-055024.

Busigny, V., Cartigny, P., Philippot, P., Ader, M., and Javoy, M., 2003, Massive recycling of nitrogen and other fluid-mobile elements (K, Rb, Cs, H) in a cold slab environment: Evidence from HP to UHP oceanic metasediments of the Schistes Lustrés nappe (western Alps, Europe): Earth and Planetary Science Letters, v. 215, p. 27–42, https://doi.org/10.1016/S0012-821X(03)00453-9.

Busigny, V., Cartigny, P., and Philippot, P., 2011, Nitrogen isotopes in ophiolitic metagabbros: A reevaluation of modern nitrogen fluxes in subduction zones and implication for the early Earth atmosphere: Geochimica et Cosmochimica Acta, v. 75, p. 7502–7521, https://doi.org/10.1016/j.gca.2011.09.049.

Cannaò, E., Tiepolo, M., Bebout, G., and Scambelluri, M., 2020, Into the deep and beyond: Carbon and nitrogen subduction recycling in secondary peridotites: Earth and Planetary Science Letters, v. 543, https://doi.org/10.1016/j.epsl.2020.116328.

Charoenpong, C.C.N., 2019, The Production and Fate of Nitrogen Species in Deep-Sea Hydrothermal Environments [Ph.D. thesis]: Cambridge, Massachusetts, Massachusetts Institute of Technology, 181 p.

Dauphas, N., and Marty, B., 1999, Heavy nitrogen in carbonatites of the Kola Peninsula: A possible signature of the deep mantle: Science, v. 286, p. 2488–2490, https://doi.org/10.1126/science.286.5449.2488.

Deschamps, F., Godard, M., Guillot, S., and Hattori, K., 2013, Geochemistry of subduction zone serpentinites: A review: Lithos, v. 178, p. 96–127, https://doi.org/10.1016/j.lithos.2013.05.019.

Grevemeyer, I., Ranero, C.R., and Ivandic, M., 2018, Structure of oceanic crust and serpentinization at subduction trenches: Geosphere, v. 14, p. 395– 418, https://doi.org/10.1130/GES01537.1.

Halama, R., Bebout, G.E., John, T., and Schenk, V., 2010, Nitrogen recycling in subducted oceanic lithosphere: The record in high- and ultrahighpressure metabasaltic rocks: Geochimica et Cosmochimica Acta, v. 74, p. 1636–1652, https://doi .org/10.1016/j.gca.2009.12.003.

Halama, R., Bebout, G.E., John, T., and Scambelluri, M., 2014, Nitrogen recycling in subducted mantle rocks and implications for the global nitrogen cycle: International Journal of Earth Sciences, v. 103, p. 2081–2099, https://doi.org/10.1007/s00531-012-0782-3.

Honma, H., and Itihara, Y., 1981, Distribution of ammonium in minerals of metamorphic and granitic rocks: Geochimica et Cosmochimica Acta, v. 45, p. 983–988, https://doi.org/10.1016/0016-7037(81)90122-8.

Johnson, B., and Goldblatt, C., 2015, The nitrogen budget of Earth: Earth-Science Reviews, v. 148, p. 150–173, https://doi.org/10.1016/j.earscirev .2015.05.006; corrigendum available at https:// doi.org/10.1016/j.earscirev.2017.01.006.

Kendrick, M.A., Hémond, C., Kamenetsky, V.S., Danyushevsky, L., Devey, C.W., Rodemann, T.,

- Jackson, M.G., and Perfit, M.R., 2017, Seawater cycled throughout Earth's mantle in partially serpentinized lithosphere: Nature Geoscience, v. 10, p. 222–228, https://doi.org/10.1038/ngeo2902.
- Lafay, R., Montes-Hernandez, G., Janots, E., Munoz, M., Auzende, A.L., Gehin, A., Chiriac, R., and Proux, O., 2016, Experimental investigation of As, Sb and Cs behavior during olivine serpentinization in hydrothermal alkaline systems: Geochimica et Cosmochimica Acta, v. 179, p. 177–202, https://doi.org/10.1016/j.gca.2016.02.014.
- Li, K., and Li, L., 2023a, Alteration enrichment of nitrogen in the gabbroic oceanic crust: Implications for global subducting nitrogen budget and subduction-zone nitrogen recycling: Geochimica et Cosmochimica Acta, v. 351, p. 96–107, https:// doi.org/10.1016/j.gca.2023.04.029.
- Li, K., and Li, L., 2023b, Nitrogen enrichment in the altered upper oceanic crust: A new perspective on constraining the global subducting nitrogen budget and implications for subduction-zone nitrogen recycling: Earth and Planetary Science Letters, v. 602, https://doi.org/10.1016/j.epsl.2022.117960.
- Li, K., Li, L., Pearson, D.G., and Stachel, T., 2019, Diamond isotope compositions indicate altered igneous oceanic crust dominates deep carbon recycling: Earth and Planetary Science Letters, v. 516, p. 190–201, https://doi.org/10.1016/j. epsl.2019.03.041.
- Li, K., Li, G.-Y., Du, Y.-F., Han, W., Zhang, J., Chen, L.-H., Zhou, J.-B., and Li, L., 2021, Intraslab remobilization of nitrogen during early subduction facilitates deep nitrogen recycling: Insights from the blueschists in the Heilongjiang Complex in NE China: Chemical Geology, v. 583, https://doi .org/10.1016/j.chemgeo.2021.120474.

- Li, L., and Bebout, G.E., 2005, Carbon and nitrogen geochemistry of sediments in the Central American convergent margin: Insights regarding subduction input fluxes, diagenesis, and paleoproductivity: Journal of Geophysical Research: Solid Earth, v. 110, B11202, https://doi.org/10.1029 /2004JB003276.
- Li, L., Bebout, G.E., and Idleman, B.D., 2007, Nitrogen concentration and $\delta^{15}N$ of altered oceanic crust obtained on ODP Legs 129 and 185: Insights into alteration-related nitrogen enrichment and the nitrogen subduction budget: Geochimica et Cosmochimica Acta, v. 71, p. 2344–2360, https://doi.org/10.1016/j.gca.2007.02.001.
- Li, L., Lollar, B.S., Li, H., Wortmann, U.G., and Lacrampe-Couloume, G., 2012, Ammonium stability and nitrogen isotope fractionations for NH₄+-NH₃(aq)-NH₃(gas) systems at 20–70° C and pH of 2–13: Applications to habitability and nitrogen cycling in low-temperature hydrothermal systems: Geochimica et Cosmochimica Acta, v. 84, p. 280–296, https://doi.org/10.1016/j.gca.2012.01.040.
- Li, L., Li, K., Li, Y., Zhang, J., Du, Y., and Labbe, M., 2021, Recommendations on offline combustionbased nitrogen isotopic analysis of silicate minerals and rocks: Rapid Communications in Mass Spectrometry, v. 35, https://doi.org/10.1002/rcm .9075.
- Li, Y.H., Li, L., and Wu, Z.Q., 2021, First-principles calculations of equilibrium nitrogen isotope fractionations among aqueous ammonium, silicate minerals and salts: Geochimica et Cosmochimica Acta, v. 297, p. 220–232, https://doi.org/10.1016/j.gca.2021.01.019.
- Marty, B., 2012, The origins and concentrations of water, carbon, nitrogen and noble gases on Earth: Earth and Planetary Science Letters, v. 313–314,

- p. 56–66, https://doi.org/10.1016/j.epsl.2011.10 .040.
- McCollom, T.M., and Bach, W., 2009, Thermodynamic constraints on hydrogen generation during serpentinization of ultramafic rocks: Geochimica et Cosmochimica Acta, v. 73, p. 856–875, https://doi.org/10.1016/j.gca.2008.10.032.
- Mével, C., and Stamoudi, C., 1996, Hydrothermal alteration of the upper-mantle section at Hess Deep, in Mével, C., Gillis, K.M., Allan, J.F., and Meyer, P.S., eds., Proceedings of the Ocean Drilling Program, Scientific Results, Volume 147: College Station, Texas, Ocean Drilling Program, p. 293–309, https://doi.org/10.2973/odp.proc.sr.147.017.1996.
- Philippot, P., Busigny, V., Scambelluri, M., and Cartigny, P., 2007, Oxygen and nitrogen isotopes as tracers of fluid activities in serpentinites and metasediments during subduction: Mineralogy and Petrology, v. 91, p. 11–24, https://doi.org/10.1007/s00710-007-0183-7.
- Sadofsky, S.J., and Bebout, G.E., 2004, Nitrogen geochemistry of subducting sediments: New results from the Izu-Bonin-Mariana margin and insights regarding global nitrogen subduction: Geochemistry, Geophysics, Geosystems, v. 5, Q03I15, https://doi.org/10.1029/2003GC000543.
- Shannon, R.T., and Prewitt, C.T., 1969, Effective ionic radii in oxides and fluorides: Acta Crystallographica B–Structural Crystallography and Crystal Chemistry, v. 25, p. 925–946, https://doi.org/10.1107/S0567740869003220.
- Sidey, V., 2016, On the effective ionic radii for ammonium: Acta Crystallographica B-Structural Science, Crystal Engineering and Materials, v. 72, p. 626–633, https://doi.org/10.1107/S2052520616008064.

Printed in the USA